Structural Imperfections in Ultrathin Silicon Oxide Film and Its Interface

Takeo HATTORI

Department of Electrical and Electronic Engineering,
Musashi Institute of Technology,
1-28-1 Tamazutsumi, Setagaya-ku, Tokyo 158, Japan

Abstracts

The structural imperfections in ultrathin silicon oxide films studied by measuring X-ray photoelectron spectra, infrared absorption spectra and reflectance spectra in vacuum ultraviolet are reviewed. The Si-H bonds, Si-OH bonds and intermediate oxidation states found in native oxides formed during wet chemical treamtents are discussed. The detection of structural transition in thermal oxide near the interface are also discussed.

1. Introduction

The operation of 0.1 m gate-length MOSFETS with gate oxide film thickness of 3.3 nm at 77 K was confirmed[1]. Because such ultrathin gate oxide film consists mostly of transition region, imperfections are introduced not only at the interface, but also in the oxide in order to relax the stress near the interface. Furthermore, the quality of the gate oxide film affects on the structural transition in silicon substrate near the interface. Therefore, the study of the imperfection in the oxide film is not only important from the insulating property of the oxide, but also from the carrier transport in silicon substrate near the interface.

It is the purpose of the present paper to review on the structural imperfections in ultrathin silicon oxide film and its interface.

2. SiO_2/Si interface structures[2]

Present understanding of SiO_2/Si interface structures can be summarized as follows: 1) The compositional transition from Si to SiO_2 takes place almost abruptly with the transition layer thickness of 1 2 molecular layers, 2) The structural transition from interface to the bulk takes place on both sides of the interface, 3) The interface is almost flat in atomic scale, 4) The small amount of suboxides exists at and near the interface, 5) The

crystalline SiO_2 exists in the oxide near the interface, 6) Pb center exists at the interface, while E' center exists in the oxide.

However, these results were not obtained for the same silicon substrates, the same oxidation methods and conditions. Therefore, these results were not consistent with each other. Furthermore, the following points were not clarified yet: 1) The chemical structures at and near the interface[3], 2) The effects of areal density of silicon atoms on the structural transition, 3) The effects of oxidation methods and conditions on the interface structure, 4) The effects of crystalline SiO_2 on the interface structure, 5) The effects of impurities on interface structure[4),5], 6) The structural imperfections in the oxide and at the interface, such as Si-H bond, Si-OH bond, 7) The surface structure of the oxide, 8) The initial oxidation mechanism, 9) The interface formation mechanism, 10) The possibility to produce ideal interface with no structural imperfections.

In the present paper the studies on 2), 6) and 7) by measuring X-ray photoelectron spectra, infrared absorption spectra, reflectance spectra in vacuum ultraviolet will be reviewed.

3. Structural imperfections in the oxide

A) Si-H bonds in native oxide[6)]

The stress near the SiO_2/Si interface is considered to relax, if the silicon atoms near the interface are terminated with hydrogen atoms. The dependence of Si-H bond density in thermal oxides on oxidation conditions and annealing was studied by measuring infrared absorption[7)]. However, the distribution of Si-H bonds near the interface could not be measured because of large probing depth in infrared absorption. In order to detemine the distribution of Si-H bonds near the interface, it is necessary to detect Si-H bonds by structure sensitive measurement with small probing depth such as XPS. However, the sensitivity of XPS is not large enough to detect extremely large amount of Si-H bonds in high quality thermal oxides. The amount of Si-H bonds in native oxides formed during wet chemical treatments are considered to be large enough to detect Si-H bonds by XPS. Actually, the Si 2p photoelectron spectrum arising from Si-H bonds could be detected to determine the distribution of Si-H bonds in the native oxides as described in the following.

The native oxides studied are that formed in a hot solution of HNO_3 and that formed in a solution of NH4OH mixed with H_2O_2 and H_2O. The details of the wet chemical treatments used to form native oxides were described elsewhere[8)].

Fig. 1 shows infrared absorption spectra measured for these two native oxides by FT-IR-ATR. According to this figure, infrared absorption arising from stretching vibration of silicon bonding to one hydrogen atom and three oxygen atoms is observed. The amount of Si-H bonds in a native oxide formed in HNO_3 is 0.25 monolayer, while that in native oxide formed in a native oxide formed in NH_4OH is 0.04 monolayer.

The Si^{x+} spectrum appears on Si 2p photoelectron spectrum for native oxide formed in HNO_3 in Fig. 2(a) and can be attributed to this Si-H bonds because of following reasons: 1) Si^{x+} is detected in a native oxide formed in HNO_3, while Si^{x+} is not detected in NH_4OH, 2) The amount of Si-H bonds estimated from Si^{x+} spectral intensity is almost equal to that estimated from the infrared absorption spectrum, 3) The binding energy of Si 2p core level for Si^{x+} calculated based on the local electronegativity[9] is close to that observed.

Fig. 3 shows the angle resolved Si 2p photoelectron spectra of native oxides formed in HNO_3 measured with angle of 6 degrees. Here, Si^{n+} corresponds to the bonding configuration of $Si-Si_{4-n}O_n$ and the intensities of Si^{4+} photoelectron spectra are ajusted to be equal to each other. Then, the almost same intensity of Si^{x+} for three take off angles implies that Si-H bonds are distributed almost

uniformly in native oxide.

B) Si-OH bonds in native oxide[10)]

Fig. 4 shows the infrared absorption spectrum measured for two kinds of native oxides by FT-IR-ATR. The amount of Si-OH in native oxides are found to be extremely small as compared to the amount of Si-H bonds estimated in A). Namely, in two kinds of native oxides studied the amount of Si-OH is nearly equal to 4×10^{-4} monolayer.

C) Intermediate oxidation states in native oxide

Fig. 5 shows the reflectance spectra in vacuum ultraviolet measured for two kinds of native oxides[11)] used in Fig. 1. As in the case of thermal oxides formed in dry oxygen at 800 and 1050 C[12,13)], the reflectance spectra of native oxides are found to be different from those of fused quartz below the fundamental optical absorption edge of fused quartz. From the Kramers-Kronig analysis considering multiple reflections at the boundaries of the films[12),13)], these discrepancies are found to be originated from the the increase in optical absorption in the films below the fundamental optical absorption edge of fused quartz as shown in Fig. 6.

The optical absorption at 7.8 eV in Fig. 6 can be attributed to Si-Si bonds in silicon oxide[14)]. The amount of

Si-Si bonds in native oxide is almost close to one monolayer as in the case of thermal oxide[15]. The Si 2p photoelectron spectrum corresponding to this Si-Si bond is now being studied in order to clarify the distribution of Si-Si bonds in the native oxide film.

D) Structural transition in thermal oxide[16,17,18]

The structural imperfections are considered to be localized in the structural transition region near the interface. The structural transition region can be probed by measuring chemical etching rate in depth direction as discussed in the following.

Fig. 7 shows the silicon dioxide film thickness as a function of chemical etching time. The silicon dioxide film thicknesses are calculated from the spectral intensity ratio (NO/NS). Here, NO and NS is the Si 2p spectral intensity of silicon in silicon dioxide and that in silicon substrate, respectively. In the case of oxide film formed in dry oxygen at 1000 C, the chemical etching rate is constant for large oxide thickness, while the etching rate becomes larger below the thickness of 5.5 nm. In the case of oxide film formed in 10 % dry oxygen diluted with dry argon at 1000 C, the etching rate becomes larger below the thickness of 3.5 nm. In the case of oxide film formed in 10 % dry oxygen diluted with dry argon at 1000 C followed by annealing in

argon at 1000 C for one hour, the etching rate does not become larger in the thickness range studied. If the transition layer thickness is assumed to be equal to the thickness below which the etching rate increases, the decrease in transition layer thickness by annealing is obtained.

Based on this assumption, the transition layer thicknesses were determined for thermal oxides formed in dry oxygen at 800 and 1000 C on (100), (110) and (111) surfaces. The areal density of silicon atom on these three surfaces is different with each other. Fig. 8 shows the dependence of silicon dioxide film thickness on chemical etching rate for thermal oxides formed on 1000 C. From this figure the transition layer thickness are found to increase with increasing areal density of silicon atom.

4. Summary and Future Problems

The studies on structural imperfections in native oxides are reviewed in addition to the structural transition in thermal oxides. The studies on structural imperfections in native oxides will be the base for the studies on structural imperfections of thermal oxides. It is shown from the measurement of infrared absorption spectra and Si 2p photoelectron spectra that the detection of Si-H bonds by XPS is possible and can be used to determine the distribution of

Si-H bonds in native oxides.

The contribution of oxidation at terrace and step to initial interface formation and the structural imperfections in thermal oxide near the interface introduced by wet chemical treatments should be clarified.

Furthermore, the correlation of SiO_2/Si interface structure with disordered-Induced gap state model[19], interstitial silicon formed during oxidation[20], pile up of impurities near the interface[21] and the existence of superstructure at the interface[22] should be clarified.

References

1) G. A. Sai-Halasz, M. R. Wordeman, D. P. Kern, E. Ganin, S. Rishton, D. S. Zicherman, H. Schmid, M. R. Polcari, H. Y. Ng, P. J. Restle, T. H. P. Chang and R. H. Dennard: IEEE Electron Device Lett. ED-8 (1987) 463.

2) C. R. Helms and B. E. Deal, ed. : The Physics and Chemistry of SiO_2 and the Si-SiO_2 Interfaces (Plenum Press, New York, 1988).

3) T. Hattori, T. Igarashi, M. Ohi and Hyamagishi: Jpn. J. Appl. Phys. 28 (1989) L1436.

4) M. Morita, T. Ohmi and E. Hasegawa: Solid-State electronics 33, suppl. (1990) 143.

5) C. Heimlich, M. Kubota, Y. Murata, T. Hattori, M. Morita and T. Ohmi: Vacuum 41 (1990) 793.

6) K. Sugiyama, T. Igarashi, K. Moriki, Y. Nagasawa, T. Aoyama, R. Sugino, T. Ito and T. Hattori: to be published in Jpn. J. Appl. Phys. Vol. 29, No. 12 (1990).

7) Y. Nagasawa, I. Yoshii, K. Naruke, K. Yamamoto, H. Ishida and A. Ishitani: J. Appl. Phys. 68 (1990) 1429.

8) T. Hattori, K. Takase, H. Yamagishi, R. Sugino, Y. Nara and T. Ito: Jpn. J. Appl. Phys. 28 (1989) L296.

9) G. Lucovsky: J. de Physique 42 (1981) C4-741.

10) K. Sugiyama, T. Igarashi, K. Moriki, Y. Nagasawa, T. Aoyama, R. Sugino, T. Ito and T. Hattori: Extended Abstracts 22nd (1990 Intern.) Conf. Solid State Devices

and Materials, Sendai, 1990 (Business Center for Academic Societies Japan, Tokyo, 1990) p.1075.

11) N. Terada, T. Haga, K. Moriki, N. Miyata, T. Aoyama, R. Sugino, M. Fujisawa and T. Hattori: to be published.

12) N. Miyata, K. Moriki, M. Fujisawa, M. Hirayama, T. Matsukawam and T. Hattori: Jpn. J. Appl. Phys. 28 (1989) L2072.

13) N. Miyata, K. Moriki, M. Hirayama, T. Matsukawa, M. Fujisawa and T. Hattori: Solid-State Electronics 33, Suppl. (1990) 327.

14) H. Imai, K. Arai, H. Imagawa, H. Hoshino and Y. Abe: Phys. Rev. B38 (1988) 12772.

15) T. Haga, N. Miyata, K. Moriki, M. Fujisawa, T. Kaneoka, M. Hirayama, T. Matsukawa and T. Hattori: to be published in Jpn. J. Appl. Phys. Vol. 29, No. 12, 1990.

16) H. Yamagishi, N. Koike, K. Imai, K. Yamabe and T. Hattori: Jpn. J. Appl. Phys. 27 (1988) L1398.

17) T. Hattori H. Yamagishi, N. Koike, K. Imai and K. Yamabe: Appl. Surf. Sci. 41/42 (1989) 416.

18) T. Hattori: Solid-State Electronics 33, suppl. (1990) 297.

19) H. Ohno and H. Hasegawa: Jpn. J. Appl. Phys. 25 (1986) L353.

20) K. Taniguchi, D. A. Antoniadis and Y. Mtushita: Appl. Phys. Lett. 42 (1983) 961.

21) T. Kimura, M. Hirose and Y. Osaka: J. Appl. Phys. 56 (1984) 932.

22) J. M. Gibson, H. -J. Gossman, J. C. Bean, R. T. Tung and L. C. Feldman: Phys. Rev. Lett. 56 (1986) 355.

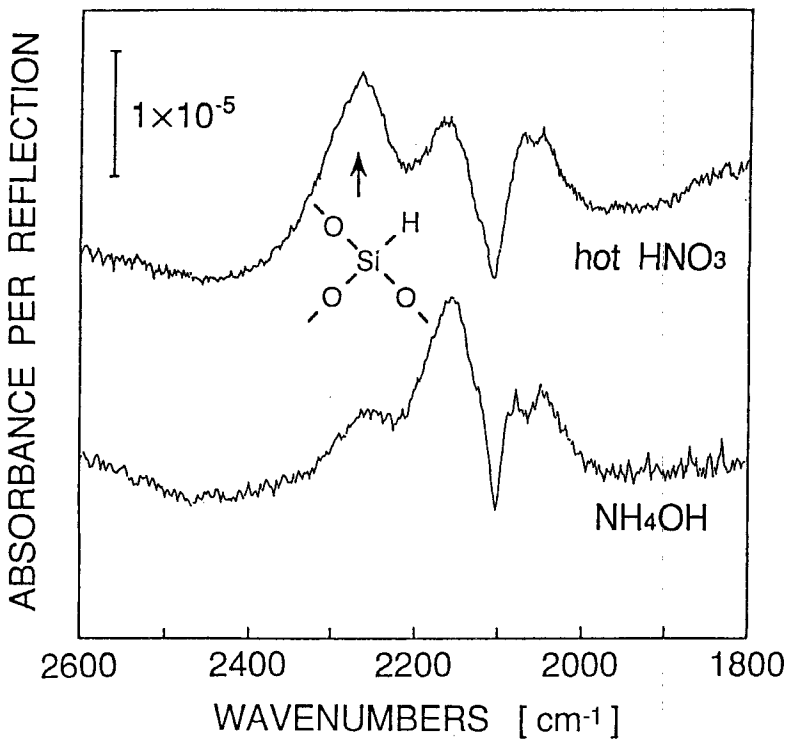

Fig. 1 Infrared absorption spectra of native oxides formed in hot HNO_3, and in NH_4OH.

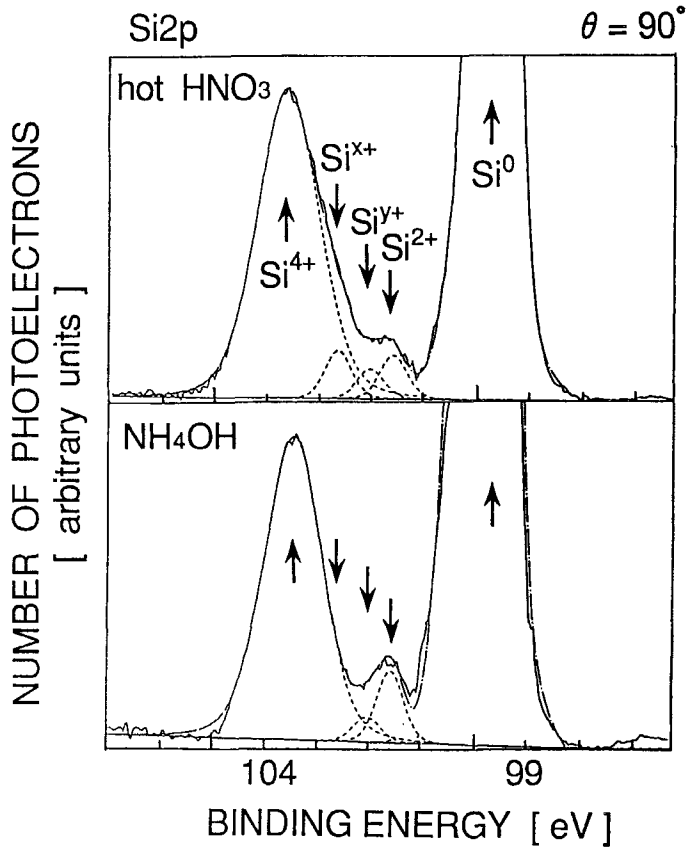

Fig. 2 Si 2p photoelectron spectra and their deconvoluted spectra obtained for native oxides formed in hot HNO_3, and in NH_4OH.

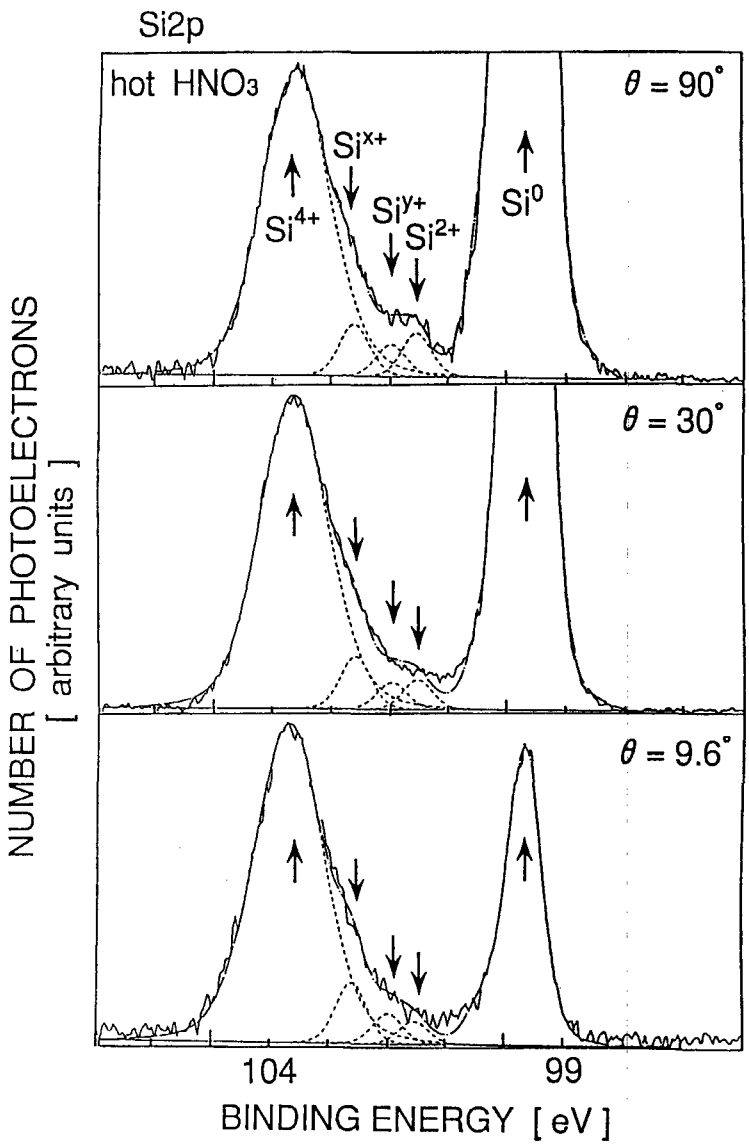

Fig. 3 Angle resolved Si 2p photoelectron spectra and their deconvoluted spectra obtained for native oxide formed in hot HNO_3 for three take off angles.

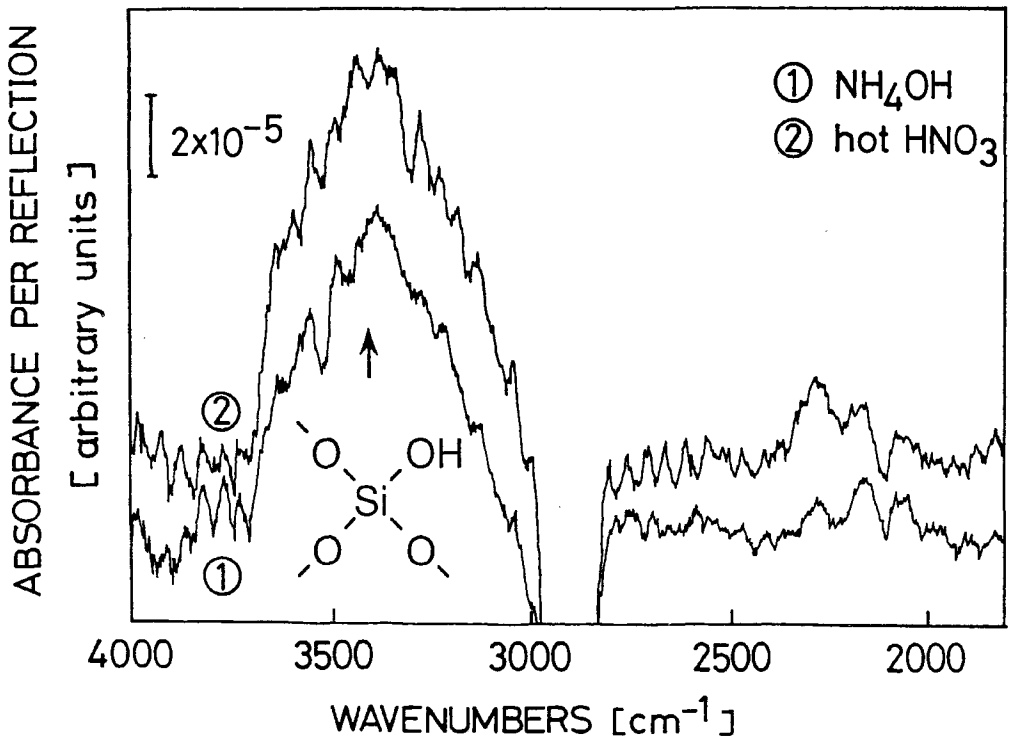

Fig. 4 Infrared absorption spectra of native oxides formed in hot HNO_3, and NH_4OH.

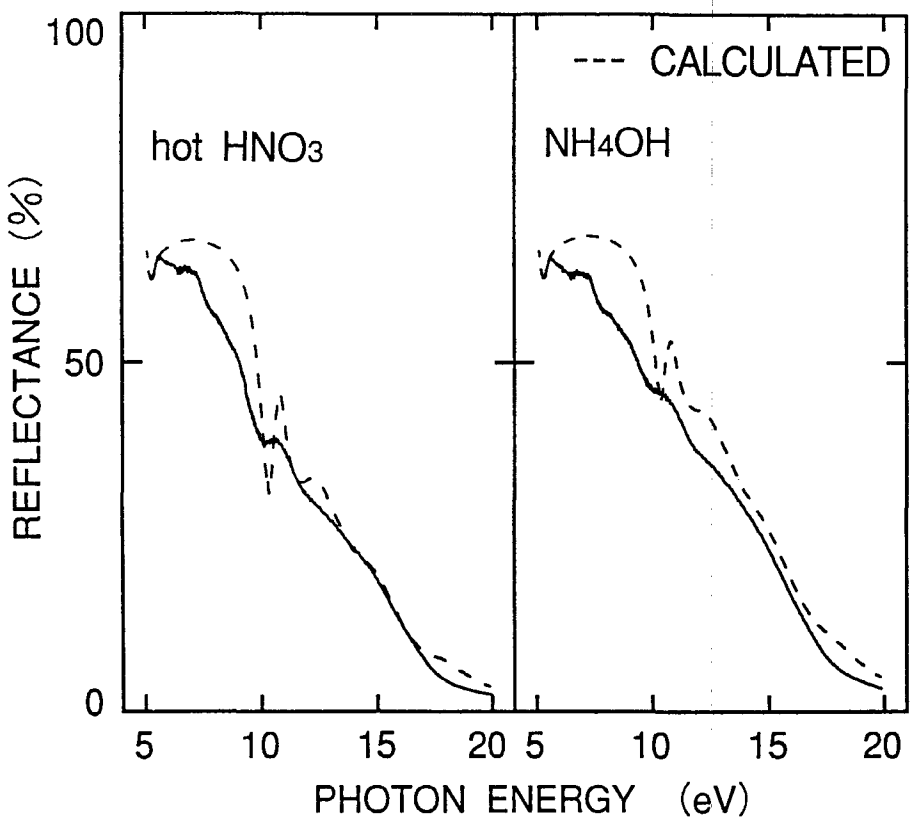

Fig. 5 Reflectance spectra in vacuum ultraviolet of native oxides formed in hot HNO_3, and NH_4OH.

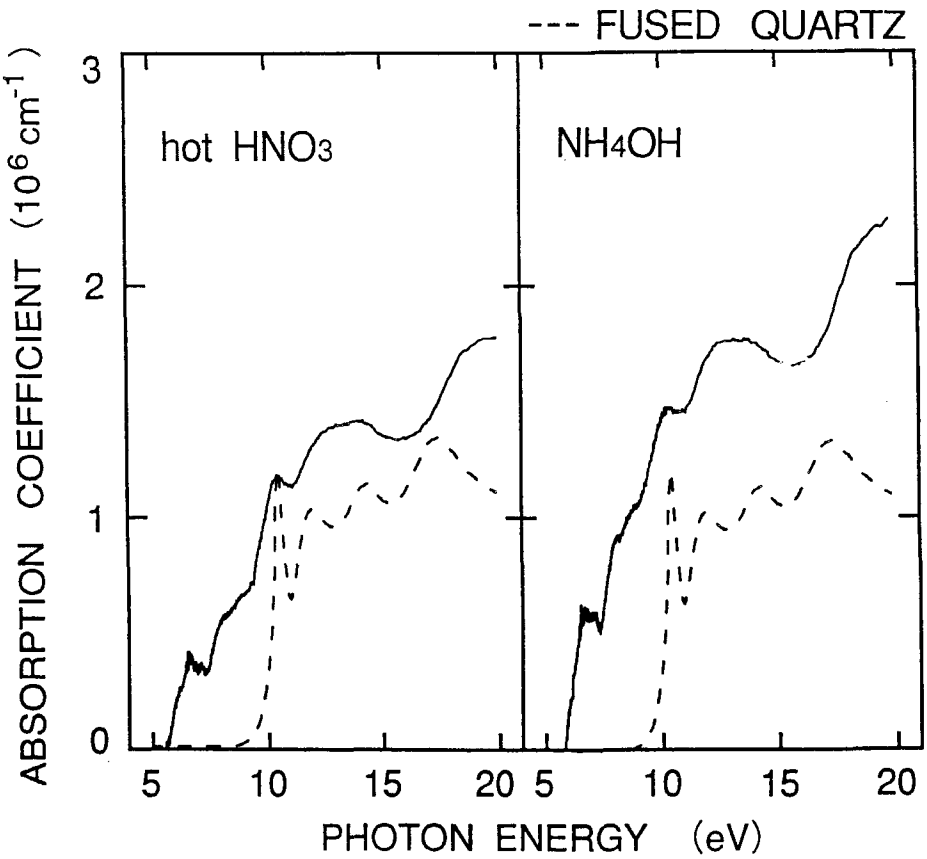

Fig. 6 Photon energy dependence of absorption coefficients obtained from the analysis of Fig. 5.

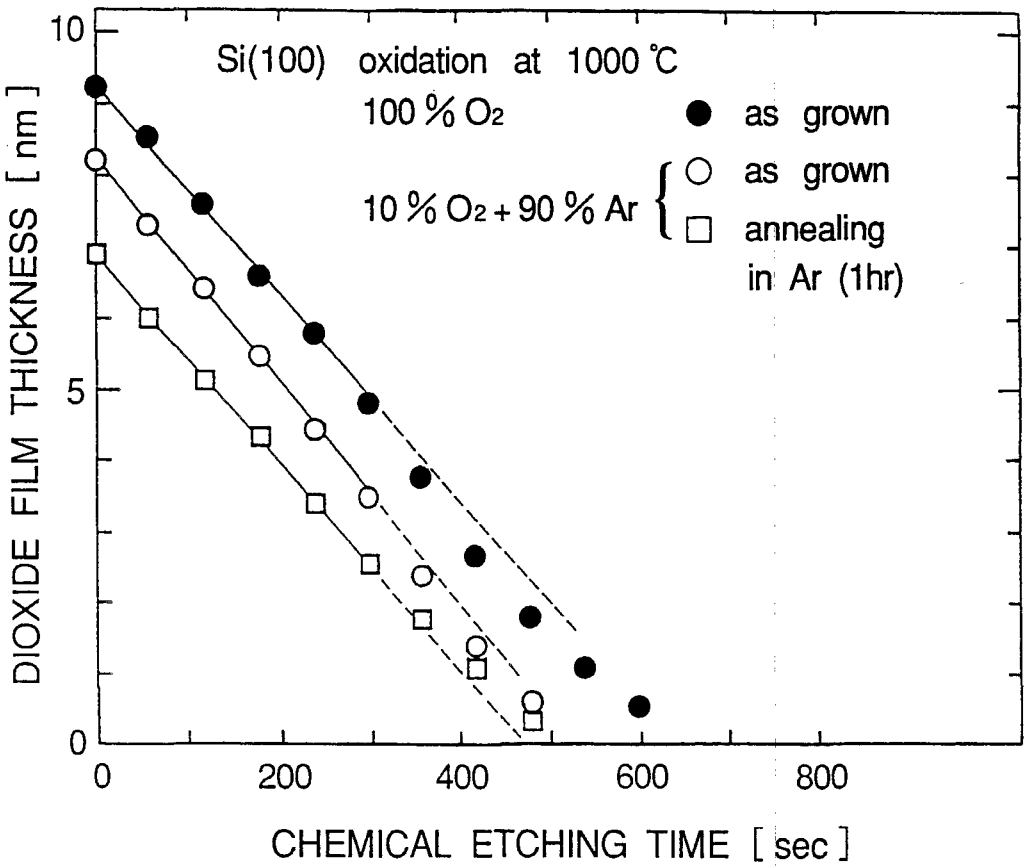

Fig. 7 Dependence of silicon dioxide film thickness on chemical etching time for three kinds of thermal oxides.

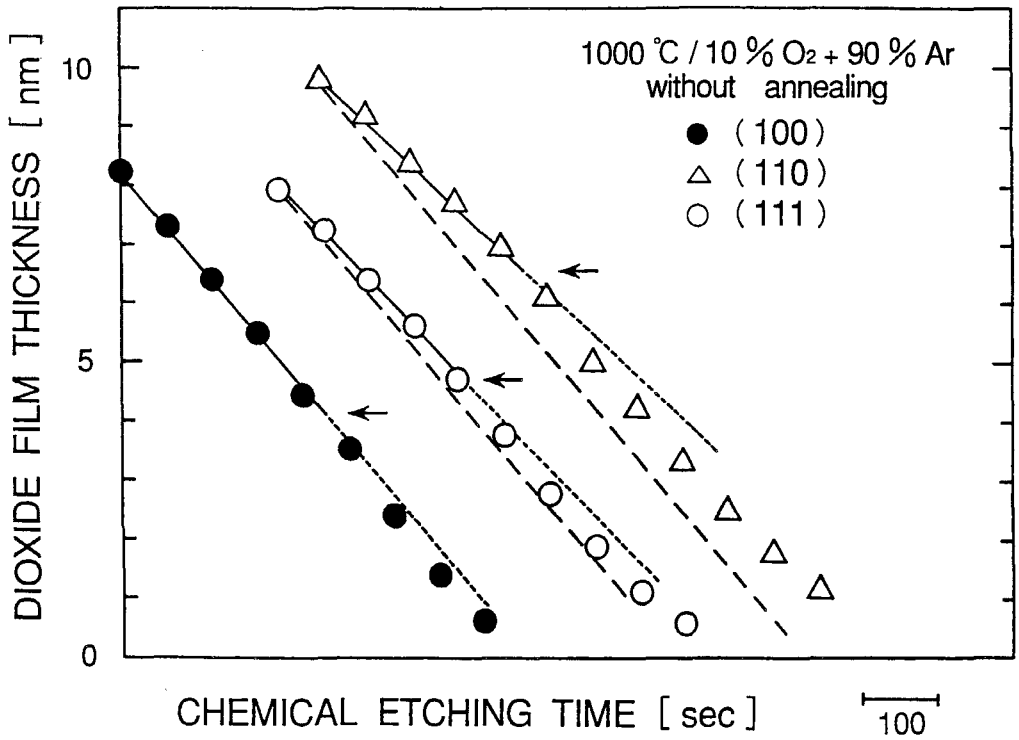

Fig. 8 Dependence of silicon dioxide film thickness on chemical etching time for thermal oxides formed on three crystallographic orientations.